ORIGINAL PAPER

Optimization parameters for electro discharge machining on Nimonic 80A alloy using grey relational analysis

Maddipati Rajesh[1] · M. Naga Swapna Sri[2] · S. Jeyakrishnan[3] · P. Anusha[2] · Javvadi Eswara Manikanta[4] · N. Sateesh[5] · B. Ch. Nookaraju[5] · Ram subbiah[5] · S. Vijayakumar[6]

Abstract

Abrasive powder-mixed electrode-coated electrical discharge machining (APMEC-EDM) is a hybrid manufacturing process that involves using a abrasive powder mixed dielectric fluid and coated electrodes and combining benefits of both mechanical and thermal interactions. Present study aims to use a new performance assessment technique, gray relational analysis (GRA), to assess the influence of optimizing the APMEC-EDM performance on Nimonic80A Superalloy. Here, five control factors are considered as machining parameters: pulse current (A), pulse on-time (T_{on}), pulse off-time (T_{off}), Inter Electrode gap (mm), and aluminum powder concentration (g/L). The GRA L27 Orthogonal Array DOE can determine best parameters for multiple responses. GRA is employed to acquire a single performance index, and gray correlational class is used to optimize the APMEC-EDM process using a gray correlation coefficient with a lower tool wear rate, radial overcut, and higher material removal rate. The multi-objective optimization optimum values are Current at 15 A, Inter Electrode Gap at 2 mm, and Powder concentration in dielectric at 9 g/l, T_{on} at 300 µs, and T_{off} at 90 µs.

Keywords APMEC-EDM · Nimonic80A · L_{27} orthogonal array · Gray correlation

1 Introduction

High strength, hardness, and impact resistance materials are in high demand in the mechanical sectors. These materials are challenging when using traditional techniques like turning, drilling, milling, etc. [1, 2]. The progress of a new invention of materials results from the search for novel, lightweight materials with better strength and durability. These characteristics can frequently pose significant difficulties while machining [3]. From its humble beginnings as an essential technique

✉ S. Jeyakrishnan
jkmech2003@gmail.com

Maddipati Rajesh
rajamaddipati61@gmail.com

M. Naga Swapna Sri
mswapnasri@pvpsiddhartha.ac.in

P. Anusha
anoosha.peyyala@gmail.com

Javvadi Eswara Manikanta
manijem66@gmail.com

N. Sateesh
Sateeshnagari1@gmail.com

B. Ch. Nookaraju
nookaraju@griet.ac.in

Ram subbiah
ram4msrm@gmail.com

S. Vijayakumar
vijaysundarbe@gmail.com

1 Research Scholar in Trans-Disciplinary Research Hub, Andhra University, Visakhapatnam, Andhra Pradesh 530003, India

2 Department of Mechanical Engineering, P V P Siddhartha Institute of Technology, Vijayawada, India

3 Department of Mechanical Engineering, ARM College of Engineering and Technology, Maraimalainagar, Chennai 603209, India

4 Department of Mechanical Engineering, Shri Vishnu Engineering College for Women (A), Bhimavaram 534202, India

5 Department of Mechanical Engineering, Gokaraju Rangaraju Institute of Engineering and Technology, Hyderabad, India

6 Department of Mechanical Engineering, BVC Engineering College (Autonomous), Odalarevu, Andhra Pradesh 533210, India

for crafting tools and dies, wire electrical discharge machining (WEDM) has undergone a remarkable transformation, emerging as the ultimate solution for fabricating micro-scale components with unparalleled precision in dimensions and surface finish [4]. An unconventional thermoelectric process called WEDM makes use of isolated sparks between the work electrode and tool electrode that are separated by a small layer of dielectric fluid to erode material from the workpiece.[5–8]. Controlled erosion can erode the metal tool by applying sparks between the metal tool and workpiece. The workpiece melts and vaporizes due to the intense thermal conditions that the spark's heat energy creates. The problem known as electrode wear (EW) occurs when the electrode melts and evaporates as a result of the elevated temperatures of the sparks [9, 10]. The EW process and the material removal mechanism are comparable since the EDM electrode and workpiece surface are viewed as electrodes. Because of this wear, electrodes get smaller, which affects how accurately cavities are created [11]. EDM's two most crucial output parameters are material removal rate (MRR) and tool wear rate (TWR). EDM is a unique metal-cutting technique for making intricate dies and mechanical components used in space vehicles, automobiles, and many other industries. [12]. Superalloys and high-strength materials are hard to cut conventionally due to tool edge chipping or fracture, tool attrition wear, and poor thermal diffusivity. Moreover, these new materials' high production costs, poor MRRs, and surface quality present challenges for traditional cutting [13]. Several machining techniques, Advanced Machining Processes (AMPs) and Non-Conventional Machining Processes (NCMP) were created to solve these problems. Advanced machining techniques like EDM remove material electrothermally [14]. Purohit et al. reported employing GRA based on taguchi to optimize process parameters, including MRR and EWR [15]. Mandalio et al. investigated the influence of many EDM process parameters utilizing Design of experiments and Regression analysis employing tungsten-thorium electrodes [16]. Mohanty et al. used particle swarm optimization to optimize further the Inconel 718 work material's numerous performance parameters for the EDM process. Tool material, pulse duration, and discharge current were discovered to impact machinability substantially [17]—Choudhary et al. compared electrodes treated with cryogenic and noncryogenic temperatures for Hastelloy EDM [18]. Compared to noncryogenic treated electrodes, it was found that tool electrodes that had undergone cryogenic treatment produced a superior surface polish. The EDM surface carbon content was discovered using a tool electrode that had yet to be cryogenically treated. Zhang et al. investigated brass tube electrode-based fabricating micro-holes with different outside diameters [19]. Sonawane and Kulkarni studied multi-objective Nimonic 75 optimization using the Taguchi method, and the principal component analysis approach

was carried out on the WEDM process. Confirmatory trials demonstrated that the SF, MRR, and overcut anticipated response values closely matched the outcomes of the experiments [20]. Vikas K. Shukla et al. reported machining performance and multi-criteria optimization of novel metal-Nimonic 80A using EDM. They identified that pulse-on time and peak current are significant parameters for MRR [21].

In this study, the MRR, TWR, and ROC performance characteristics were multi-objectively optimized by varying possible input process parameters over a specified range in the EDM process. This study examines grey relational analysis based on Taguchi for multi-objective optimization of machining properties of EDM on Nimonic-80A. This research contributes to advanced machining by addressing the challenges associated with high-strength materials, offering innovative solutions, and presenting a comprehensive approach to multi-objective optimization in the EDM process on Nimonic-80A.

2 Materials and experimental setup

In EDM, tool material plays a very vital role in the Machining. In this present study, a Copper electrode coated with Silver (3 μ) thickness is used. The electrode dimensions are 10 mm in diameter and 50 mm in length, respectively. In this present study, Nimonic 80A serves as the work material. The dimensions of rectangular workpiece material are 15 mm*5 mm. Figure 1 shows the electrode and workpiece. The powder used in the present study is Aluminum metal powder of 325 meshes, which is used to mix in the dielectric—aluminum powder concentration in the dielectric ranges from 3 to 9 g/l.

All experiments used an EDM model ARD ARTM30D (Die-sinking type). The dielectric fluid employed was white kerosene. The EDM machine tool can be observed in Fig. 1. Aluminum powder is added to the dielectric to examine the effect on responses. As the powder concentration is taken as one of the input variables, it is not easy to maintain the total tank with a 200 L capacity. To minimize this, a separate tray of 1 l capacity was prepared, and the different concentration levels were examined. The workpieces are fitted with the help of Glue.

3 Cutting condition and experimental design

The selection of optimal EDM machining characteristics is a crucial component. Taguchi Optimization is a single-parameter optimization method centered upon that signal-to-noise ratio [22]. GRA improves parameters with many outcomes using grey relational grade [23]. ANOVA is also

Fig. 1 a Workpiece and electrode, **b** EDM setup, **c** Arrangement of workpieces
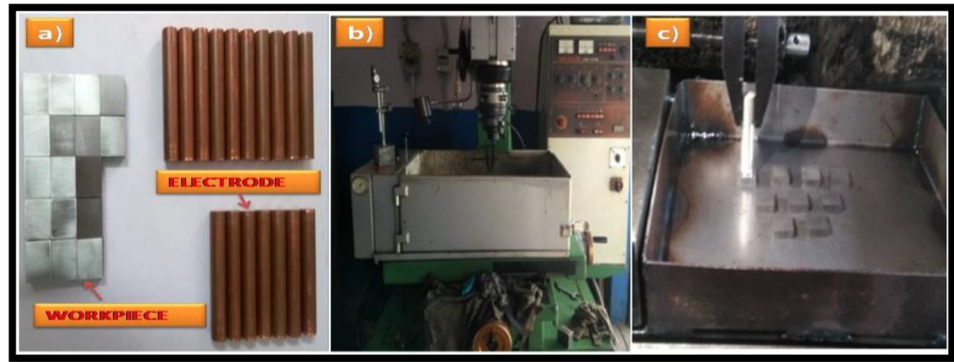
Table 1 Process parameters levels

Process parameters	Units	Levels		
Current	A	3	9	15
Pulse on time (t_{on})	μs	300	600	900
Pulse off time (t_{off})	μs	30	60	90
Inter electrode gap	mm	1	2	3
Aluminum powder concentration	g/l	3	6	9

conducted to ascertain whether process factors are statistically significant [24–26]. The process parameters chosen and the levels of the variables are tabulated in Table 1. The response variables affected concerning the process parameters are Material Removal Rate (MRR), Tool Wear rate (TWR), and Radial overcut (ROC). The Experiments were carried out in accordance with L27 OA using a random approach generated using MINITAB. A different electrode (Silver Coated Copper Electrode) is used for each experiment. The machining time considered for Nimonic 80A is 5 min. The arrangement of the experiments according to the L27 Orthogonal array is tabulated in Table 2 with the actual values.

4 Results and discussions

The experiments were conducted on all the 27 specimens with 5 min of machining time. The specimens and the electrodes are to be weighed before and after conducting the experiments. The electrode's diameter at the tip of the machining and the hole diameter produced are to be measured for every specimen using vernier calipers. The weights and Diameters measured before and after the experiments are tabulated. The response variables (MRR, TWR, ROC) are calculated and are tabulated. Table 3 displays measured weights, tool, and workpiece diameter, and the measured response variables. The Eqs. (1–13) for calculation are given below.

Material Removal Rate (MRR):

$$MRR = \frac{W_b - W_a}{t} \; g/min \tag{1}$$

Tool Wear Rate (TWR):

$$TWR = \frac{W_{tb} - W_{ta}}{t} \; g/min \tag{2}$$

Radial over Cut (ROC):

$$C = \frac{D_h - D_t}{2} \; mm \tag{3}$$

Where W_b & W_a = Weight of the workpiece prior to and after Machining. W_{tb} & W_{ta} = Weight of Tool Prior to and after Machining. D_t & D_h = Diameter of Tool and Hole respectively. t = time taken for Machining.

Any process must use the optimum process parameter combination to get desired output response while utilizing the fewest resources possible. The Analysis of Variance (ANOVA) approach is employed for calculating the Optimum Response Variables and the Effect of Process Parameters on the Response Variables.

5 Calculation of S/N ratio for MRR

Taguchi's signal-to-noise ratio is the logarithmic function of the intended output.. The S/N ratio is the mean-to-standard

Table 2 Design of experiments with actual value

DOE	IEG (mm)	Current (A)	Powder concentration (g/l)	On time (μs)	Off time (μs)
1	1	5	3	300	30
2	1	5	3	300	60
3	1	5	3	300	90
4	1	12	6	600	30
5	1	12	6	600	60
6	1	12	6	600	90
7	1	15	9	900	30
8	1	15	9	900	60
9	1	15	9	900	90
10	2	5	6	900	30
11	2	5	6	900	60
12	2	5	6	900	90
13	2	12	9	300	30
14	2	12	9	300	60
15	2	12	9	300	90
16	2	15	3	600	30
17	2	15	3	600	60
18	2	15	3	600	90
19	3	5	9	600	30
20	3	5	9	600	60
21	3	5	9	600	90
22	3	12	3	900	30
23	3	12	3	900	60
24	3	12	3	900	90
25	3	15	6	300	30
26	3	15	6	300	60
27	3	15	6	300	90

deviation ratio. The term mean relates to the signal, and standard deviation refers to the noise. The quality of the product or process being optimized determines the value of this ratio [27]. As the material removal rate is the response, which is to be maximum, the larger is better will be considered in calculating the S/N ratios. The Higher the MRR indicates that the machining performance will be maximum. The computed values of "Larger the Better S/N ratios" for MRR in negative signs are tabulated [28].

$$\left(\frac{S}{N}\right)_{HB} = -10 log_{10}(MSD_{HB}) dB \qquad (4)$$

$$MSD_{HB} = \frac{1}{n} \sum_{i=1}^{n} \frac{1}{Y_i^2} \qquad (5)$$

6 Calculation of S/N ratio for TWR

A low tool rate will permit an increase in the tool's life, which means the tool can be used for extended periods without changing the accuracy while machining. The sound-to-noise ratios for the TWR are found to be smaller, the better. The sound-to-noise ratios for TWR are calculated and tabulated.

$$\left(\frac{S}{N}\right)_{LB} = -10 log_{10}(MS D_{LB}) dB \qquad (6)$$

$$MSD_{LB} = \frac{1}{n} \sum_{i=1}^{n} \frac{1}{Y_i^2} \qquad (7)$$

7 Calculation of S/N ratio for ROC

Radial overcut is an error which is generated during the machining. It shouldn't be large as it may result in the

Table 3 Response values

DOE	W_b (g)	W_A (g)	MRR (g/min)	W_tb (g)	W_ta (g)	TWR (g/min)	D_t (mm)	D_h (mm)	ROC (mm)
1	11.123	11.087	0.0072	34.689	34.673	0.0032	9.920	9.933	0.0067
2	11.163	11.123	0.008	34.868	34.820	0.0096	9.870	9.917	0.0233
3	11.132	11.096	0.0072	34.826	34.812	0.0028	9.860	9.877	0.0083
4	11.119	10.992	0.0254	34.761	34.743	0.0036	9.870	9.910	0.02
5	11.087	10.942	0.029	34.726	34.697	0.0058	9.930	10.007	0.0383
6	11.047	10.826	0.0442	34.774	34.736	0.0076	9.940	9.980	0.02
7	11.149	11.033	0.0232	34.796	34.727	0.0138	9.950	10.060	0.055
8	11.093	10.914	0.0358	34.829	34.801	0.0056	9.840	9.967	0.0633
9	11.104	10.881	0.0446	34.735	34.718	0.0034	9.930	9.867	- 0.0317
10	11.094	11.071	0.0046	34.791	34.773	0.0036	9.950	9.980	0.015
11	11.152	11.131	0.0042	34.759	34.751	0.0016	9.920	10.083	0.0817
12	11.173	11.150	0.0046	34.718	34.704	0.0028	9.940	9.840	- 0.05
13	11.156	10.703	0.0906	34.788	34.770	0.0036	9.970	10.120	0.075
14	11.171	10.590	0.1162	34.727	34.719	0.0016	9.920	10.120	0.1
15	11.093	10.570	0.1046	34.798	34.760	0.0076	9.930	10.013	0.0417
16	11.129	10.932	0.0394	34.489	34.461	0.0056	9.830	9.940	0.055
17	11.167	10.759	0.0816	34.776	34.737	0.0078	9.940	10.113	0.0867
18	11.089	10.585	0.1008	34.673	34.641	0.0064	9.960	10.123	0.0817
19	11.106	11.076	0.006	34.820	34.789	0.0062	9.850	9.767	- 0.0417
20	11.122	11.096	0.0052	34.812	34.784	0.0056	9.910	9.880	- 0.015
21	11.156	11.128	0.0056	34.743	34.713	0.006	9.910	9.553	- 0.1783
22	11.100	10.936	0.0328	34.697	34.668	0.0058	9.950	10.000	0.025
23	11.153	10.974	0.0358	34.736	34.707	0.0058	9.900	10.057	0.0783
24	11.078	10.904	0.0348	34.727	34.698	0.0058	9.930	10.090	0.08
25	11.121	10.618	0.1006	34.801	34.771	0.006	9.900	10.157	0.1283
26	11.091	10.341	0.15	34.718	34.687	0.0062	9.940	10.133	0.0967
27	11.087	10.246	0.1682	34.773	34.742	0.0062	9.950	10.130	0.09

improper contours. The smaller the better formula was utilized to calculate the S/N Ratio's for the Radial Overcut and these values are presented in a table. (Table 4)

$$\left(\frac{S}{N}\right)_{LB} = -10 log_{10}(MSD_{LB}) dB \qquad (8)$$

$$MSD_{LB} = \frac{1}{n} \sum_{i=1}^{n} \frac{1}{Y_i^2} \qquad (9)$$

MSD = Mean Square Data.
Y_i = Response value of i_{th} experiment,
n = Number of Replicants.

8 Effect of process parameters on MRR

The extent to which the input variables affect the responses is to be identified. This is done by generating the response table using Minitab 18 Statistical Software [29–32]. The Main effects plot is generated by taking the input variables with 3 levels in the Abcissa and Response variable (MRR) on the ordinate. (Fig. 2)

The process parameters thus selected should be in such a way that MRR should be maximum. The levels at which the process parameters give maximum MRR are generated using Taguchi's technique. The obtained values are tabulated in response Tables. (Table 5)

Rankings are generated for various process parameters at distinct levels. The maximum values of the levels are considered as the MRR follows the Larger the better concept. The optimized parameters for MRR are Current is15 A, T_{on} =

Table 4 S/N ratios of MRR, TWR & ROC

DOE	Powder concentration	IEG	Current	T_{on}	T_{off}	MRR S/N	TWR S/N	ROC S/N
1	3	1	6	300	30	−42.853	49.8970	43.52183
2	3	1	6	300	60	−41.938	40.3545	32.64046
3	3	1	6	300	90	−42.853	51.0568	41.58362
4	3	2	12	600	30	−31.903	48.8739	33.9794
5	3	2	12	600	60	−30.752	44.7314	28.32847
6	3	2	12	600	90	−27.092	42.3837	33.9794
7	3	3	15	900	30	−32.69	37.2024	25.19275
8	3	3	15	900	60	−28.922	45.0362	23.96735
9	3	3	15	900	90	−27.013	49.3704	55.56303
10	6	2	6	900	30	−46.745	48.8739	36.47817
11	6	2	6	900	60	−47.535	55.9176	21.7591
12	6	2	6	900	90	−46.745	51.0568	43.52183
13	6	3	12	300	30	−20.857	48.8739	22.49877
14	6	3	12	300	60	−18.696	55.9176	20
15	6	3	12	300	90	−19.609	42.3837	27.60422
16	6	1	15	600	30	−28.09	45.0362	25.19275
17	6	1	15	600	60	−21.766	42.1581	21.24296
18	6	1	15	600	90	−19.931	43.8764	21.7591
19	9	3	6	600	30	−44.437	44.1521	41.58362
20	9	3	6	600	60	−45.68	45.0362	34.73517
21	9	3	6	600	90	−45.036	44.4369	55.56303
22	9	1	12	900	30	−29.683	44.7314	32.0412
23	9	1	12	900	60	−28.922	44.7314	22.12107
24	9	1	12	900	90	−29.168	44.7314	21.9382
25	9	2	15	300	30	−19.948	44.4369	17.83321
26	9	2	15	300	60	−16.478	44.1521	20.29447
27	9	2	15	300	90	−15.484	44.1521	20.91515

Fig. 2 Main effects plot for MRR
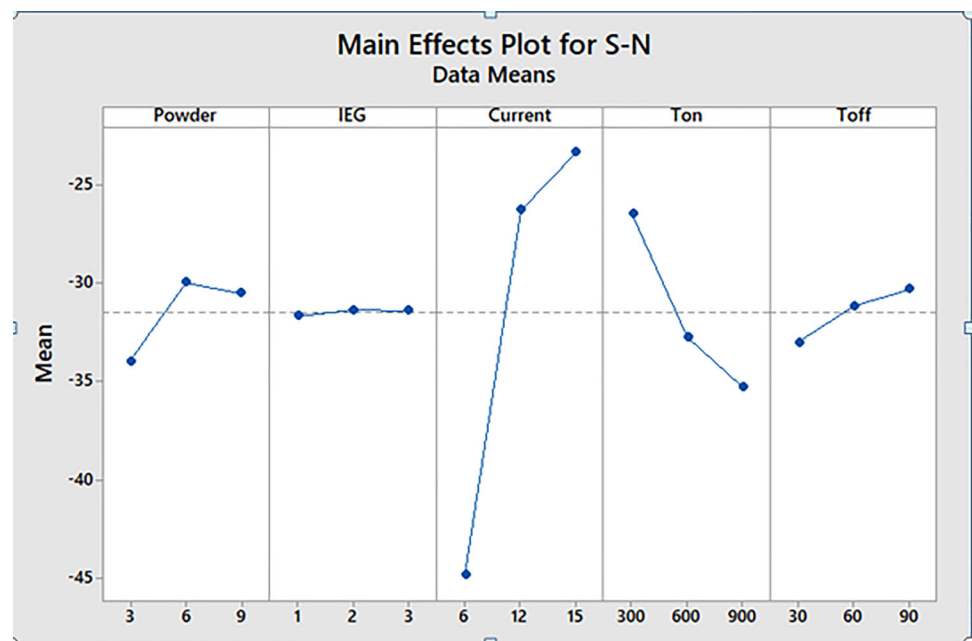
Table 5 Response table for MRR

Level	Response Table for Signal to noise ratios				
	P C (g/l)	IEG (mm)	Current (A)	T_{on} (µs)	T_{off} (µs)
1	−34	−31.69	−44.87	−26.52	−33.02
2	−30	−31.41	−26.3	−32.74	−31.19
3	−30.54	−31.44	−23.37	−35.27	−30.33
Delta	4	0.28	21.5	8.75	2.7
Rank	3	5	1	2	4

Table 6 Response table for TWR

Level	Response table for signal to noise ratios				
	IEG (mm)	T_{on} (µs)	Current (A)	T_{off} (µs)	P C (g/l)
1	−33.08	−33.36	−33.56	−33.18	−33.1
2	−33.44	−32.96	−33.29	−33.29	−33.62
3	−33.17	−33.36	−32.84	−33.22	−32.97
Delta	0.37	0.4	0.73	0.1	0.65
Rank	4	3	1	5	2

300 µs, Powder concentration is 6 g/l, T_{off} is 90 µs and IEG is 2 mm. (Table 6)

9 Effect of process parameters on TWR:

The optimized parameters for TWR are Current is 12 A, Powder concentration is 3 g/l, T_{on} is 300 µs, IEG is 1 mm and T_{off} is 30 µs. (Table 7)

10 Effect of process parameters on ROC

Rankings are generated for various process parameters at distinct levels. The minimum values of levels are considered as the TWR follows the smaller the better concept. The optimized parameters for ROC are Current is 6 A, Powder Concentration is 3 g/l, T_{off} is 90 µs, T_{on} is 600 µs and IEG is 3 mm. (Figs. 3), 4

11 ANOVA for response variable

ANOVA, a statistical method, is employed to discover variations in average performance of the test set of items [33, 34]. ANOVA at a 95% confidence interval can be used to specify the significant impact of process factors on response parameters. A Two-way ANOVA was employed to generate mean square value and sum of squares. F and P values are thus generated. The contribution table is also generated using ANOVA in Minitab. (Tables 8, 9, 10)

If the *P* value is below 0.05, they are considered to affect the response variable significantly. Thus, the Percentage contributions of the process parameters on the response variables are found. Significant ANOVA percentage of contribution for MRR, current is the primary factor, contributing 91.06%. In TWR variance analysis, current dominates, contributing 34.81%. Current is the foremost factor in ROC variance analysis, contributing 37.94%.

12 Multi objective optimization by grey relational analysis (GRA)

Any process must use the optimum process parameter combinations to achieve the desired output response while utilizing the fewest resources possible. The ideal parameter choice for one response may harm other replies.

In order to determine the best parameter configuration, it is necessary to find a middle ground and conduct multi-objective optimization [25]. Over the years, many optimization approaches have evolved to optimize the parameters by solving numerous objective functions [26]. One such technique is GRA. Multiple performance characteristics have been explored using the Grey Relational technique in Grey Relational Analysis. GRA allows the examination of multiple performance attributes, converting them into a unified metric known as the Grey Relational Grade (GRG). The GRG plays a vital role in grey relational analysis as it demonstrates the connection between sequences. When both sequences are identical, the GRGe value is 1. Moreover, the GRG indicates the impact of the comparison sequence on the reference
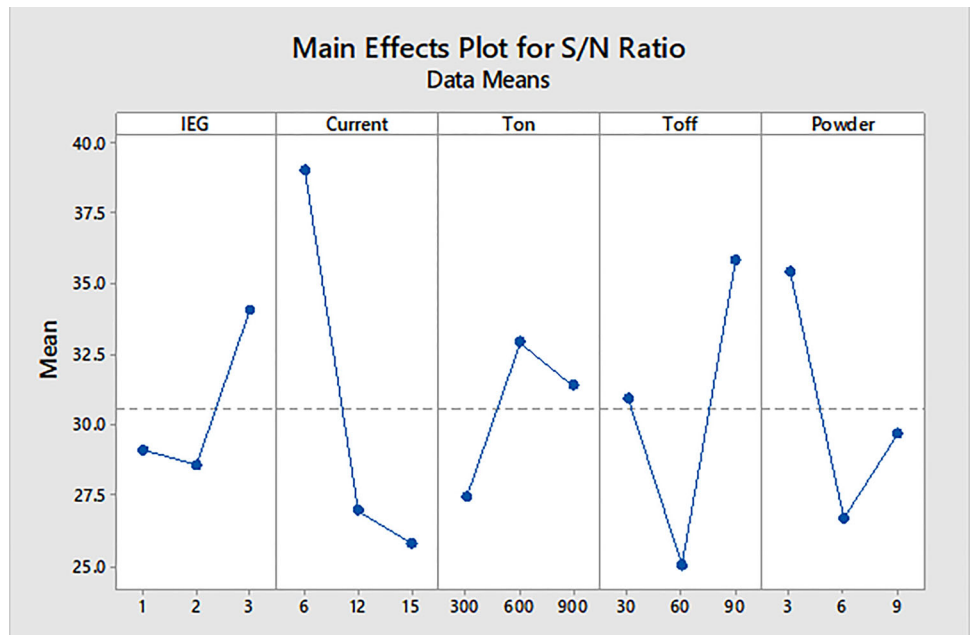
Table 7 Response table for ROC

Response Table for Signal to Noise Ratios					
Level	IEG (mm)	Current (A)	T_{on} (μs)	T_{off} (μs)	P C (g/l)
1	29.12	39.04	27.43	30.92	35.42
2	28.57	26.94	32.93	25.01	26.67
3	34.08	25.77	31.4	35.83	29.67
Delta	5.51	13.27	5.5	10.82	8.74
Rank	4	1	5	2	3

Fig. 3 Main effects plot for TWR
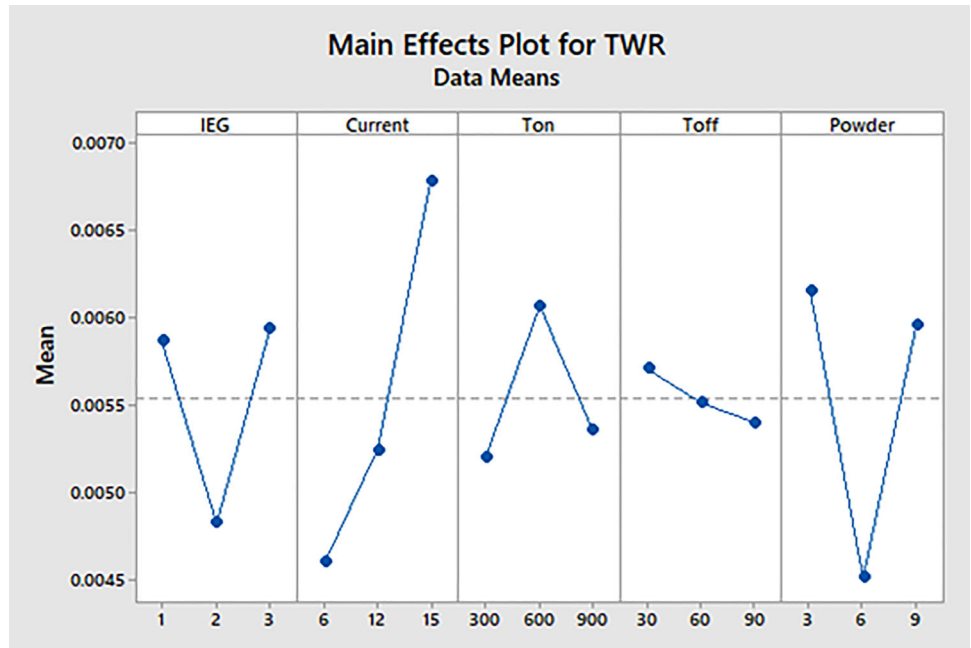
Fig. 4 Main effects plot for roc

Table 8 ANOVA for MRR

Source	DF	Seq SS	Contribution	Adj SS	Adj MS	F-Value	P value
Powder concentration (g/l)	2	0.797	0.15%	0.797	0.398	1.42	0.27
IEG (mm)	2	3.037	0.58%	3.037	1.518	5.42	0.016
Current (A)	2	480.5	91.06%	480.5	240	857	0
Pulse on Time (μs)	2	36.89	6.99%	36.89	18	65.8	0
Pulse off Time (μs)	2	1.941	0.37%	1.941	0.97	3.46	0.056
Error	16	4.485	0.85%	4.485	0.28		
Total	26	527.684	100.00%				

Table 9 ANOVA for TWR

Source	DF	Seq SS	Contribution	Adj SS	Adj MS	F-Value	P value
Powder concentration (g/l)	2	8.9767	24.16%	8.9767	4.4884	1.89	0.0183
IEG (mm)	2	0.2485	3.92%	0.24857	0.1242	0.52	0.602
Current (A)	2	10.9385	34.81%	10.9385	5.4692	1.98	0.0171
Pulse on Time (μs)	2	6.423	16.67%	6.423	3.2115	0.89	0.043
Pulse off Time (μs)	2	0.0286	0.45%	0.02867	0.0143	0.06	0.0942
Error	16	3.8011	19.98%	3.8011	0.2375		
Total	26	6.3376	100.00%				

Table 10 ANOVA for ROC

Source	DF	Seq SS	Contribution	Adj SS	Adj MS	F-Value	P value
IEG (mm)	2	0.000978	2.74%	0.000978	0.000489	1.08	0.364
Current (A)	2	0.013553	37.94%	0.013553	0.006777	14.94	0
Pulse on Time (μs)	2	0.003339	9.35%	0.003339	0.00167	3.68	0.048
Pulse off Time (μs)	2	0.003984	11.15%	0.003984	0.001992	4.39	0.03
Powder concentration (g/l)	2	0.006608	18.50%	0.006608	0.003304	7.29	0.006
Error	16	0.007257	20.32%	0.007257	0.000454		
Total	26	0.035719	100.00%				

sequence. Therefore, when a specific comparison sequence exerts a more substantial influence on the reference sequence compared to others, its GRG with the reference sequence will be greater than the GRGs of the others.

Normalizing the S/N values For higher the better

$$Z_{ij} = \frac{y_{ij} - \min\left(y_{ij}, i = 1, 2, \ldots n\right)}{\max\left(y_{ij}, i = 1, 2, \ldots n\right) - \min\left(y_{ij}, i = 1, 2, \ldots n\right)} \quad (10)$$

Normalizing the S/N values For Smaller the better

$$Z_{ij} = \frac{\min\left(y_{ij}, i = 1, 2, \ldots n\right) - y_{ij}}{\max\left(y_{ij}, i = 1, 2, \ldots n\right) - \min\left(y_{ij}, i = 1, 2, \ldots n\right)} \quad (11)$$

The highest and lowest values for MRR, TWR & ROC are taken respectively in the Eqs. 10 and 11 for normalization. The normalized values are tabulated in Table 11.

Table 11 Grey relational coefficient

DOE	Normalizing the S/N values			Deviation sequence			Grey relational coefficient		
	MRR	TWR	ROC	MRR	TWR	ROC	MRR	TWR	ROC
1	0.1461	0.3217	0.3191	0.8539	0.6783	0.6809	0.3693	0.4243	0.4234
2	0.1746	0.8316	0.6075	0.8254	0.1684	0.3925	0.3773	0.7480	0.5603
3	0.1461	0.2597	0.3705	0.8539	0.7403	0.6295	0.3693	0.4031	0.4427
4	0.4877	0.3764	0.5721	0.5123	0.6236	0.4279	0.4939	0.4450	0.5388
5	0.5236	0.5977	0.7218	0.4764	0.4023	0.2782	0.5121	0.5541	0.6425
6	0.6378	0.7231	0.5721	0.3622	0.2769	0.4279	0.5799	0.6436	0.5388
7	0.4632	1	0.8049	0.5368	0	0.1951	0.4822	1	0.7194
8	0.5807	0.5814	0.8374	0.4193	0.4186	0.1626	0.5439	0.5443	0.7546
9	0.6403	0.3498	0	0.3597	0.6502	1	0.5816	0.4347	0.3333
10	0.0247	0.3764	0.5058	0.9753	0.6236	0.4942	0.3389	0.4450	0.5029
11	0	0	0.8959	1	1	0.1041	0.3333	0.3333	0.8277
12	0.0247	0.2597	0.3191	0.9753	0.7403	0.6809	0.3389	0.4031	0.4234
13	0.8323	0.3764	0.8763	0.1677	0.6236	0.1237	0.7489	0.4450	0.8017
14	0.8998	0	0.9426	0.1002	1	0.0574	0.8330	0.3333	0.8970
15	0.8713	0.7231	0.741	0.1287	0.2769	0.2590	0.7953	0.6436	0.6588
16	0.6067	0.5814	0.8049	0.3933	0.4186	0.1951	0.5597	0.5443	0.7194
17	0.804	0.7352	0.9096	0.1960	0.2648	0.0904	0.7184	0.6538	0.8469
18	0.8612	0.6434	0.8959	0.1388	0.3566	0.1041	0.7828	0.5837	0.8277
19	0.0967	0.6287	0.3705	0.9033	0.3713	0.6295	0.3563	0.5738	0.4427
20	0.0579	0.5814	0.552	0.9421	0.4186	0.4480	0.3467	0.5443	0.5274
21	0.078	0.6134	0	0.9220	0.3866	1	0.3516	0.5640	0.3333
22	0.557	0.5977	0.6234	0.4430	0.4023	0.3766	0.5302	0.5541	0.5704
23	0.5807	0.5977	0.8864	0.4193	0.4023	0.1136	0.5439	0.5541	0.8148
24	0.573	0.5977	0.8912	0.4270	0.4023	0.1088	0.5394	0.5541	0.8213
25	0.8607	0.6134	1	0.1393	0.3866	0	0.7821	0.5640	1
26	0.969	0.6287	0.9348	0.0310	0.3713	0.0652	0.9416	0.5738	0.8846
27	1	0.6287	0.9183	0	0.3713	0.0817	1	0.5738	0.8596

Calculation of Grey Relational Coefficient

$$\xi_i(k) = \frac{\Delta_{min} + \zeta\Delta_{max}}{\Delta_{Oi}(k) + \zeta\Delta_{max}} \tag{12}$$

where Δ is the Deviation sequence, Where $\Delta_{0i}(k)$ is the deviation sequence of the reference sequence and compatibility sequence. ζ is identified coefficients. The value of ζ is the lesser and recognized ability is the larger. $\zeta = 0.5$ is usually utilized.

Calculation of GRG

$$\gamma_i = \frac{1}{n}\sum_{k=1}^{n}\xi_i(k) \tag{13}$$

The Grey Relational grades are ranked as per their value and are tabulated in Table 12. The ideal solution for getting the Maximum MRR, Minimum TWR, and ROC is represented by rank 1. The optimized properties thus obtained are Current at 15 A, Inter Electrode Gap at 2 mm, Powder concentration in dielectric at 9 g/l, Pulse on time at 300 µs &Pulse off time at 90 µs.

13 Microstructure analysis

The optical microstructure analysis of EDM performed on Nimonic 80A alloy reveals critical insights into the material's structural changes. Under the EDM process, the alloy's microstructure exhibits distinct characteristics, including recast layers and micro-cracks formation. The recast layers, composed of re-solidified material, can vary in thickness based on EDM parameters such as pulse energy, duration, and sparking frequency. Micro-cracks indicate localized

**Table 12** Grey relational coefficient and ranking of GRG for the design of experiments

DOE	Powder concentration (g/l)	IEG (mm)	Current (A)	T_{on} (µs)	T_{off} (µs)	MRR	TWR	ROC	GRG	Rank
1	3	1	6	300	30	0.3693	0.4243	0.4234	0.4057	25
2	3	1	6	300	60	0.3773	0.7480	0.5603	0.5618	16
3	3	1	6	300	90	0.3693	0.4031	0.4427	0.4050	26
4	3	2	12	600	30	0.4939	0.4450	0.5388	0.4926	19
5	3	2	12	600	60	0.5121	0.5541	0.6425	0.5696	15
6	3	2	12	600	90	0.5799	0.6436	0.5388	0.5875	14
7	3	3	15	900	30	0.4822	1	0.7194	0.7339	5
8	3	3	15	900	60	0.5439	0.5443	0.7546	0.6143	12
9	3	3	15	900	90	0.5816	0.4347	0.3333	0.4499	22
10	6	2	6	900	30	0.3389	0.4450	0.5029	0.4289	23
11	6	2	6	900	60	0.3333	0.3333	0.8277	0.4981	18
12	6	2	6	900	90	0.3389	0.4031	0.4234	0.3885	27
13	6	3	12	300	30	0.7489	0.4450	0.8017	0.6652	9
14	6	3	12	300	60	0.8330	0.3333	0.8970	0.6878	8
15	6	3	12	300	90	0.7953	0.6436	0.6588	0.6992	7
16	6	1	15	600	30	0.5597	0.5443	0.7194	0.6078	13
17	6	1	15	600	60	0.7184	0.6538	0.8469	0.7397	4
18	6	1	15	600	90	0.7828	0.5837	0.8277	0.7314	6
19	9	3	6	600	30	0.3563	0.5738	0.4427	0.4576	21
20	9	3	6	600	60	0.3467	0.5443	0.5274	0.4728	20
21	9	3	6	600	90	0.3516	0.5640	0.3333	0.4163	24
22	9	1	12	900	30	0.5302	0.5541	0.5704	0.5516	17
23	9	1	12	900	60	0.5439	0.5541	0.8148	0.6376	11
24	9	1	12	900	90	0.5394	0.5541	0.8213	0.6383	10
25	9	2	15	300	30	0.7821	0.5640	1	0.7820	3
26	9	2	15	300	60	0.9416	0.5738	0.8846	0.8000	2
27	9	2	15	300	90	1	0.5738	0.8596	0.8111	1

material removal, demonstrating the EDM process's thermal influence. Studying these optical microstructures provides valuable information for optimizing EDM parameters and understanding how they impact the surface quality and material properties of Nimonic 80A alloy components. Figure 5 reveals a significant presence of surface defects, including excessive melted material deposition, microcracks, clusters of debris globules, as well as micro-pores on the machined surface, where an aluminum powder concentration of 9 g/L was introduced, displays a noticeable reduction in surface defects compared to aluminum powder concentration of 3 g/L. The enhancement in surface morphology becomes more pronounced, incorporating an aluminum powder concentration of 6 g/L, demonstrating a substantial decrease in surface defects.

Figure 5 shows a significant decrease in the deposition of molten material and the occurrence of micro-cracks, debris globules, and micro-pores. The introduction of aluminum powder has significantly mitigated surface defects. These nanoparticles promote consistent sparking between work and tool interface, effectively diminishing micro-cracks. Furthermore, it widens the IEG and enhances the heat dissipation of the dielectric fluid through the formation of small craters, thereby reducing plasma heat flux and mitigating issues related to melted material deposition and globule formation, as well as micro-pore formation. Adding aluminum powder also facilitates improved debris flushing within the machining zone, forming smaller ridges and an overall enhancement in surface quality. These Micro pores likely correspond to points where individual discharges penetrated deeply into the workpiece. When a high-energy pulse is applied, it could potentially vaporize a substantial quantity of metal during the initial discharge. Following smaller current discharges, the initial removal of metal may be less, but a larger portion is heated to its melting point and subsequently redeposited

Fig. 5 Optical microstructure of EDM on Nimonic 80A Alloy, **a** Sample 1 **b** Sample 5, **c** Sample 12, **d** Sample 20
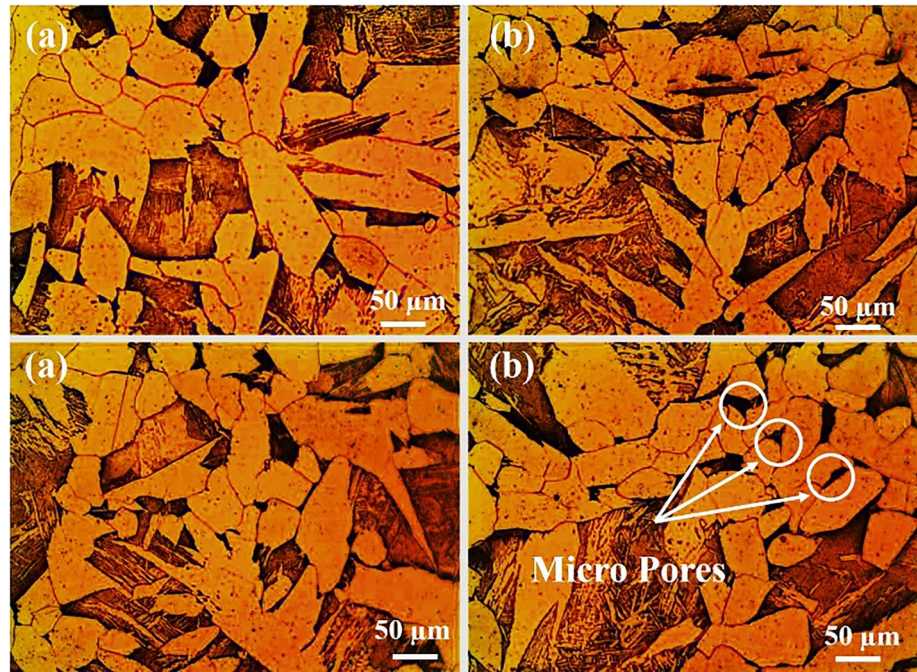
on the surface as a recast layer. Moreover, multiple built-up layers can be observed.

Increasing pulse-on time produces more powerful explosions and higher discharge energy production. This, in turn, enhances material removal rates (MRR) but also speeds the consumption of the brass wire. Residual brass wire particles can adhere to the cutting surface, resulting in rougher surfaces. Higher peak currents amplify the influence of discharge energy on the workpiece surface, exacerbating erosion and deterioration of surface roughness.

14 Conclusions

In this research, the effects of machining response are MRR, TWR, and ROC of NIMONIC 80A with silver-coated copper electrode have been investigated using the EDM process by varying IEG, Powder concentration in dielectric, Current, Pulse On time, and Pulse OFF time. GRA is used to optimize the process parameters for MRR, TWR, and ROC combined effects. From the experimental investigation, the following conclusions were drawn:

Current is the most predominant parameter on Material Removal Rate (0.168 g), Tool Wear Rate (0.013 g), and Radial Over Cut (0.128 mm).
For MRR, the best process parameters are Current at 15 A, T_{on} at 300 µs, Powder concentration in dielectric at 6 g/l, T_{off} at 90 µs, and IEG at 2 mm.

The best process parameters to obtain the minimum tool wear rate are Current at 15 A, Powder concentration in dielectric at 9 g/l, T_{on} at 600 µs, IEG at 1 mm, and T_{off} at 30 µs.
The best process parameters to obtain the minimum radial overcut Current at 6 A, Powder concentration in dielectric at 3 g/l, T_{off} at 90 µs, T_{on} at 600 µs, and IEG at 3 mm.
Multi-objective optimization is carried out using Grey Relational Analysis, yielding the optimal values as follows: Current-15 A, Inter Electrode Gap-2 mm, and Powder concentration in dielectric—9 g/l, T_{on}—300 µs and T_{off}—90 µs.

Data availability The conclusions drawn from this research study rely on the data that has been integrated into the article. Should further data or supplementary details be required, interested parties can contact the corresponding author to acquire them.

Declarations

Conflict of interest The authors declare that there are no conflicts of interest associated with the publication of this manuscript.

References

1. Zaman, U.K.U., Khan, U.A., Aziz, S., Baqai, A.A., Butt, S.U., Hussain, D., Siadat, A., Jung, D.W.: Optimization of wire electric

discharge machining (WEDM) process parameters for AISI 1045 medium carbon steel using Taguchi design of experiments. Materials **15**(21), 7846 (2022). https://doi.org/10.3390/ma15217846

2. Rath, D., Chandra Padhi, P., Kumar, S., Singh, I., Nagaprasad, N., Krishnaraj, R.: Wedm process optimization for machining characteristics of AISI 52100 grade alloy steel. Adv. Mater. Sci. Eng. **2022**, 1–12 (2022). https://doi.org/10.1155/2022/6316799

3. Perumal, A., Kailasanathan, C., Stalin, B., Suresh Kumar, S., Rajkumar, P.R., Gangadharan, T., Venkatesan, G., Nagaprasad, N., Dhinakaran, V., Krishnaraj, R.: Multiresponse optimization of wire electrical discharge machining parameters for Ti-6Al-2Sn-4Zr-2Mo (α-β) alloy using Taguchi-grey relational approach. Adv. Mater. Sci. Eng. **2022**, 1–13 (2022). https://doi.org/10.1155/2022/6905239

4. Kumar, A., Grover, N., Manna, A., Kumar, R., Chohan, J.S., Singh, S., Singh, S., Pruncu, C.I.: Multi-objective optimization of WEDM of aluminum hybrid composites using AHP and genetic algorithm. Arab. J. Sci. Eng. **47**(7), 8031–8043 (2022). https://doi.org/10.1007/s13369-021-05865-4

5. Kumar, V., Jangra, K.K., Kumar, V., Sharma, N.: WEDM of nickel based aerospace alloy: optimization of process parameters and modelling. Int. J. Interact. Des. Manuf. (IJIDeM) **11**(4), 917–929 (2017). https://doi.org/10.1007/s12008-016-0298-3

6. Durairaj, M., Sudharsun, D., Swamynathan, N.: Analysis of process parameters in wire EDM with stainless steel using single objective Taguchi method and multi objective grey relational grade. Proc. Eng. **64**, 868–877 (2013). https://doi.org/10.1016/j.proeng.2013.09.163

7. Shrinivas Balraj, U., Gopala Krishna, A.: Multi-objective optimization of EDM process parameters using Taguchi method, principal component analysis and grey relational analysis. Int. J. Manuf. Mater. Mech. Eng. **4**(2), 29–46 (2014)

8. Guu, Y.H., Hocheng, H.: Effects of workpiece rotation on machinability during electrical-discharge machining. Mater. Manuf. Processes **16**(1), 91–101 (2001). https://doi.org/10.1081/amp-100103699

9. Singh, B.P., Singh, J., Singh, K., Kalra, C.S.: *Optimizing WEDM Parameters for Machining of Nimonic-80A alloy using RSM Technique*. Ripublication.com. Retrieved August 2, 2023, from https://www.ripublication.com/ijaer18/ijaerv13n21_04.pdf (n.d.)

10. Kumar, D., Mondal, S.: Process parameters optimization of AISI M2 steel in EDM using Taguchi based TOPSIS and GRA. Mater. Today Proc. **26**, 2477–2484 (2020). https://doi.org/10.1016/j.matpr.2020.02.527

11. Choudhary, R., Gupta, V.K., Batra, Y., Singh, A.: Performance and surface integrity of nimonic75 alloy machined by electrical discharge machining. Mater. Today Proc. **2**(4–5), 3481–3490 (2015). https://doi.org/10.1016/j.matpr.2015.07.324

12. Manohar, M., Selvaraj, T., Sivakumar, D., Gopinath, S., George, K.M.: Experimental study to assess the effect of electrode bottom profiles while machining inconel 718 through EDM process. Proc. Mater. Sci. **6**, 92–104 (2014). https://doi.org/10.1016/j.mspro.2014.07.011

13. Durante, S., Rutelli, G., Rabezzana, F.: Aluminum-based MMC machining with diamond-coated cutting tools. Surf. Coat. Technol. **94–95**, 632–640 (1997). https://doi.org/10.1016/s0257-8972(97)00521-5

14. Singh, S., Maheshwari, S., Pandey, P.C.: Some investigations into the electric discharge machining of hardened tool steel using different electrode materials. J. Mater. Process. Technol. **149**(1–3), 272–277 (2004). https://doi.org/10.1016/j.jmatprotec.2003.11.046

15. Purohit, R., Rana, R.S., Dwivedi, R.K., Banoriya, D., Singh, S.K.: Optimization of electric discharge machining of M2 tool steel using grey relational analysis. Mater. Today Proc. **2**(4–5), 3378–3387 (2015). https://doi.org/10.1016/j.matpr.2015.07.312

16. Mandaloi, G., Singh, S., Kumar, P., Pal, K.: Effect on crystalline structure of AISI M2 steel using tungsten–thorium electrode through MRR, EWR, and surface finish. Meas. J. Int. Meas. Confed. **90**, 74–84 (2016). https://doi.org/10.1016/j.measurement.2016.04.041

17. Goswami, A., Kumar, J.: Investigation of surface integrity, material removal rate and wire wear ratio for WEDM of Nimonic 80A alloy using GRA and Taguchi method. Eng. Sci. Technol. Int. J. **17**(4), 173–184 (2014). https://doi.org/10.1016/j.jestch.2014.05.002

18. Choudhary, R., Garg, H., Prasad, M., Kumar, D.: Effect of cryogenic treatment of tool electrode on the machining performance and surface finish during electrical discharge machining of hastelloy C-4. Mater. Today Proc. **4**(2), 1158–1166 (2017). https://doi.org/10.1016/j.matpr.2017.01.132

19. Zhang, Y., Xu, Z., Xing, J., Zhu, D.: Effect of tube-electrode inner diameter on electrochemical discharge machining of nickel-based superalloy. Chin. J. Aeronaut. **29**(4), 1103–1110 (2016). https://doi.org/10.1016/j.cja.2015.12.016

20. Sonawane, S.A., Kulkarni, M.L.: Optimization of machining parameters of WEDM for Nimonic-75 alloy using principal component analysis integrated with Taguchi method. J. King Saud Univ. Eng. Sci. **30**(3), 250–258 (2018). https://doi.org/10.1016/j.jksues.2018.04.001

21. Shukla, V.K., Kumar, R., Singh, B.K.: Evaluation of machining performance and multi criteria optimization of novel metal-Nimonic 80A using EDM. SN Appl. Sci. **3**, 309 (2021). https://doi.org/10.1007/s42452-020-04083-1

22. Kumar, R.: *Experimental investigation of process parameters and optimization in EDM using Taguchi method and grey relational analysis*. Pnrsolution.org. Retrieved August 2, 2023, from http://pnrsolution.org/Datacenter/Vol5/Issue1/16.pdf (n.d.)

23. Jain, S., et al.: Optimization of processing variables of friction stir welded dissimilar composite joints of AA6061 and AA7075 using response surface methodology. J. Adhes. Sci. Technol. (2023). https://doi.org/10.1080/01694243.2023.2243682

24. Mishra, R.S., Jain, S.: Parametric optimization of FSWed dissimilar composite joints of AA7075 and AA6061 using RSM. Trans. Indian Inst. Met. (2023). https://doi.org/10.1007/s12666-023-02996-0

25. Jain, S., Sharma, N., et al.: Dissimilar alloys (AA6082/AA5083) joining by FSW and parametric optimization using Taguchi, grey relational and weight method. Eng. Solid Mech. (2018). https://doi.org/10.5267/j.esm.2017.10.003

26. Mishra, R., Jain, S.: Friction stir welding (FSW) process on aluminum alloy 6082–T6 using Taguchi technique. Int. J. Res. Eng. Inno. **3**, 301–305 (2019)

27. Gugulothu, B., Saminathan, R., Pradeep, A., Sharma, A., Vijayakumar, S., Paramasivam, P., Srinivasa Rao, N.: Investigating the strength of butt-welded joints of AA6082 and AA5052 alloys through friction stir welding; the impact of tool tilt angle and feed rate. J. Adhes. Sci. Technol. (2023). https://doi.org/10.1080/01694243.2023.2253631

28. Sharma, P., Paramasivam, P., Bora, B.J., Sivasundar, V.: Application of nanomaterials for emission reduction from diesel engines powered with waste cooking oil biodiesel. Int. J. Low-Carbon Technol. **18**, 795–801 (2023). https://doi.org/10.1093/ijlct/ctad060

29. Vijayakumar, S., Arunkumar, A., Pradeep, A., Satishkumar, P., Singh, B., Rama Raju, K.S., Sharma, V.K.: Optimization of process variables for shielded metal arc welding dissimilar mild steel and medium carbon steel joints. J. Adhes. Sci. Technol. (2023). https://doi.org/10.1080/01694243.2023.2227461

30. Anusha, P., Sri, M.N.S., Vijayakumar, S., Rao, T.V.J., Paramasivam, P., Jeyakrishnan, S., Saxena, K.K.: Design and optimization the wear characteristics for Al7178/TiO2/B4C/FA central hybrid composite. Int. J. Interact. Des. Manuf. (IJIDeM) (2023). https://doi.org/10.1007/s12008-023-01341-5

31. Vijayakumar, S., Satheesh Kumar, P.S., Sampath Kumar, P., Manickam, S., Ramaiah, G.B., Pydi, H.P.: The effect of stir-squeeze casting process parameters on mechanical property and density of aluminum matrix composite. In: Khan M.A. (ed.) Advances in Materials Science and Engineering (Vol. 2022, pp. 1–10). Hindawi Limited (2022). https://doi.org/10.1155/2022/3741718

32. Boopathy, G., Vanitha, V., Karthiga, K., Gugulothu, B., Pradeep, A., Pydi, H.P., Vijayakumar, S.: Optimization of tensile and impact strength for injection moulded nylon 66/SiC/B4c composites. J. Nanomater. (2022). https://doi.org/10.1155/2022/4920774

33. Manickam, S., Pradeep, A., Vijayakumar, S., Mosisa, E.: Optimization of arc welding process parameters for joining dissimilar metals. Mat. Today Proc. (2022). https://doi.org/10.1016/j.matpr.2022.06.548

34. Paramasivam, P., Vijayakumar, S.: Mechanical characterization of aluminium alloy 6063 using destructive and non-destructive testing. Mater. Today Proc. (2021). https://doi.org/10.1016/j.matpr.2021.04.312